Original Article

Dual-energy computed tomography in reducing the effective radiation dose of computed tomography urography in patients with urinary calculi

Fengying Liang[1], Ruming Zhou[2], Gang Wang[3], Yanqin Lan[4], Shaoyang Lei[4], Shuqian Zhang[4]^

[1]Department of Radiology, Affiliated Hospital of Chengde Medical College, Chengde, China; [2]Department of Nuclear Medicine, Hebei General Hospital, Shijiazhuang, China; [3]Department of Urology, Hebei General Hospital, Shijiazhuang, China; [4]Department of Radiology, Hebei General Hospital, Shijiazhuang, China

Contributions: (I) Conception and design: F Liang, G Wang, S Zhang; (II) Administrative support: R Zhou, Y Lan, S Zhang; (III) Provision of study materials or patients: R Zhou, Y Lan, G Wang; (IV) Collection and assembly of data: F Liang; (V) Data analysis and interpretation: R Zhou, G Wang, S Lei, S Zhang; (VI) Manuscript writing: All authors; (VII) Final approval of manuscript: All authors.

Correspondence to: Shuqian Zhang. Department of Radiology, Hebei General Hospital, 348 Heping West Road, Shijiazhuang 050051, China. Email: 1247225465@qq.com.

Background: To evaluate the diagnostic performance of split-bolus single-phase dual-energy computed tomography (DECT) with virtual non-contrast computed tomography (VNCT) compared to three-phase computed tomography (CT) urography in patients with urinary calculi, and to examine the performance of split-bolus single-phase DECT when reducing the effective dose.

Methods: A total of 48 patients with abdominal pain or hematuria suggestive of unilateral urinary calculi were enrolled and randomly divided into the experimental and control groups, with 24 cases in each group. Patients in the experimental group underwent split-bolus single-phase DECT to obtain a mixed nephrographic excretory phase. Patients in the control group accepted a single-bolus three-phase CT urography scan (non-contrast, nephrographic phase, and excretory phase). The CT values and the contrast-to-noise ratio (CNR) of 7 segments of the urinary tract were measured and compared between the two groups by using the Mann–Whitney U test. The dose-length product (DLP) and effective dose of each patient were compared between the two groups using an independent *t*-test.

Results: Among all 48 patients, 35 calculi were detected in the experimental group (n=24), and 47 calculi were detected in the control group (n=24). There was no significant difference between the two groups in both CT value measurements and the CNR. The mean DLP and mean effective dose of the experimental group were significantly lower than those of the control group, and the effective dose in the experimental group was decreased by 40% compared with the control group.

Conclusions: The application of DECT combined with split-bolus nephrographic excretory phase CT urography can reveal the urinary calculi covered by a contrast medium and also reduce the effective dose exposure to patients.

Keywords: Tomography; X-ray computed; dual-energy imaging; computed tomography urography (CTU); urolithiasis; radiation dose

Submitted Apr 13, 2022. Accepted for publication Aug 11, 2022. Published online Aug 15, 2022.
doi: 10.21037/qims-22-372
View this article at: https://dx.doi.org/10.21037/qims-22-372

^ ORCID: 0000-0002-3750-382X.

Introduction

Urolithiasis is a common disease among adults that has shown a steadily increasing incidence in recent years (1). Computed tomography urography (CTU) is a widely accepted imaging modality for the evaluation of suspected urinary calculi (2). It can provide key diagnostic information, including the position, shape, and size of calculi, the degree of urinary obstruction, the state of renal function, and that of the entire urinary tract after postprocessing reconstruction. Nonetheless, CTU exposes patients to high radiation doses because this examination commonly requires three-phase computed tomography (CT) scans, which are non-contrast CT, nephrographic phase CT, and excretory phase CT. Additionally, intravenous contrast mediums are usually administrated in CTU to enhance the imaging performance (3). Therefore, much research has been devoted to reducing the radiation dose incurred during three-phase CTU (4,5).

Dual-energy computed tomography (DECT) is helpful in characterizing the morphology, size, and number of the urinary calculi and in providing material-specific information that is unavailable in three-phase CTU. Moreover, DECT can reconstruct virtual non-contrast CT (VNCT) from raw data sets of contrast-enhanced DECT using low energy and high energy, which can be generated in many ways, including fast-kilovolt-peak switching and two X-ray tubes with two separate detectors. We hypothesized that single-phase DECT with the split-bolus technique could not only display the urinary calculi covered by contrast medium in VNCT images but also play an important role in reducing the effective dose of the abdomen and pelvis.

The purpose of this study was to evaluate the diagnostic performance of split-bolus single-phase DECT with VNCT compared with three-phase CTU in patients with urinary calculi and to explore its performance in reducing the effective dose of the abdomen and pelvis.

Methods

Patients

The study was conducted in accordance with the Declaration of Helsinki (as revised in 2013) and was approved by Hebei General Hospital Ethics Committee (No. 2022054). Informed consent was provided by all individual participants. Between January 2020 and December 2020, a total of 48 consecutive patients who applied for CTU examination due to abdominal pain and hematuria were enrolled in this study. After signing the informed consent form, all patients were randomly allocated to either the experimental group or control group using a randomized digital table, with 24 cases in each group. The inclusion criteria were as follows: (I) abdominal ultrasonography that had suggested unilateral urinary calculi, causing unilateral hydronephrosis or ureterectasia; (II) an estimated glomerular filtration rate (eGFR) >60 mL/min; (III) no contraindication for furosemide; (IV) systolic blood pressure >90 mmHg; and (V) the ability to get on and off the examination table freely. The exclusion criteria were as follows: (I) ultrasonography findings indicative of renal, ureter, or bladder neoplasm; (II) serum creatinine >111 μmol/L; (III) images of poor quality or containing image artifacts.

Imaging protocol

The CT imaging was performed using a DECT scanner (Discovery CT750HD; GE Medical Systems, Milwaukee, WI, USA). All participants consumed 500–1,000 mL of water 30–60 minutes before the CT scan and were administrated 20 mg/2 mL of furosemide 20 minutes before the scan (6). All participants were administrated a total dose of 90 mL of ioversol (320 mg/mL; Hengrui Medicine, Jiangsu, China).

Patients in the experimental group underwent single-phase DECT with split-bolus technology using a high-pressure syringe (Zenith-C11; Seacrown Electromechanical, Shenzhen, China). With this technique, a fractionated dose of contrast medium (40 mL) was administrated at a rate of 2 mL/s followed by a delay of 15–30 minutes before the remaining contrast medium (50 mL) was given at a rate of 3 mL/s. A subsequent scan in gemstone spectral imaging (GSI) mode, obtained 75 seconds after the second dose of contrast medium and 40 mL of intravenous normal saline, showed a mixed nephrographic excretory phase. The parameters were as follows: tube potential switched between 80 and 140 kVp within 0.5 ms; tube current, 550 mAs; tube rotation time, 0.6 s; pitch, 0.984:1; detector width, 40 mm; scan slice thickness, 5 mm; slice spacing, 5 mm; reconstruction slice thickness, 1.25 mm; and field of view (FOV), 350 mm × 350 mm. The scans ranged from the bilateral adrenal glands to the level of the pubic symphysis.

Patients in the control group underwent single-bolus three-phase CTU. A non-contrast CT scan was initially performed. Then, a total dose of 90 mL of contrast medium was administrated intravenously by a high-pressure injector

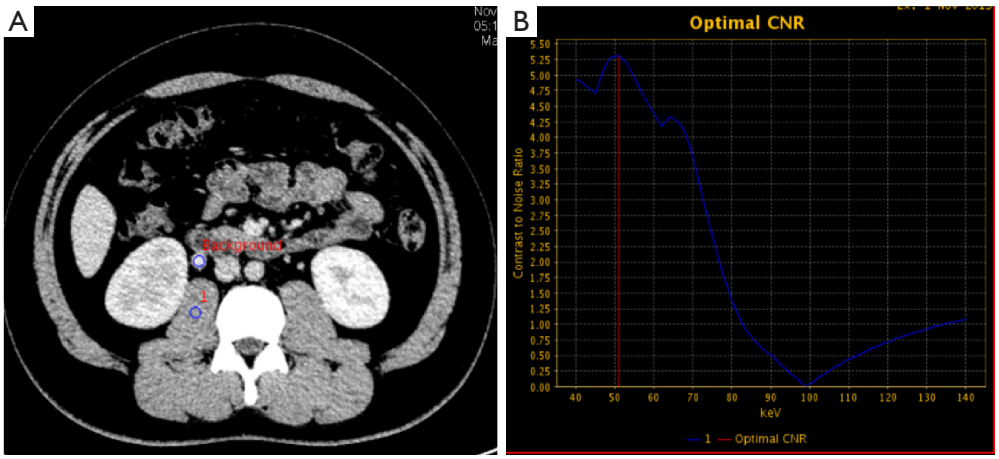

Figure 1 Optimal single energy acquisition. The axial CT image shows a mixed nephrographic excretory phase from the experimental group (A). The CNR curve was generated by setting two regions of interest (blue circle) in the ureteral lumen of the upper urinary tract and the psoas major, representing background and soft tissue, respectively. The highest point (51 keV) of the CNR curve cultivated from 40–140 keV represented the optimal single energy for the urinary tract (B). CT, computed tomography; CNR, contrast-to-noise ratio.

at a rate of 2.5 mL/s, followed by 40 mL of sodium chloride at the same rate. After a delay of 50 seconds, nephrographic phase CT was performed, followed by another delay of 15–30 minutes before excretory phase CT was performed. Three acquisitions were performed with the adaptive statistical iterative reconstruction (ASiR) scan mode of DECT. The parameters were set as follows: tube potential, 120 kV; automatic tube current modulation; tube rotation time, 0.6 s; pitch, 0.984:1; detector width, 40 mm; scan slice thickness, 5 mm; slice spacing, 5 mm; and FOV, 350 mm × 350 mm. The scanning range of each phase was the same as that of the experimental group.

Image analysis

All raw image data were reconstructed with a slice thickness of 1.25 mm, and images from the experimental group were required to reconstruct monochromatic (Mono) images with a slice thickness of 1.25 mm. Then, all images were transferred to Advantage Workstation (AW) 4.4 (GE Healthcare, Chicago, IL, USA) for postprocessing analysis.

All dual-energy data of the nephrographic excretory phase from the experimental group were presented in the GSI Viewer (GE Healthcare). These data required two postprocessing steps. First, two isometric regions of interest (ROIs) were placed in the ureteral lumen of the upper urinary tract and the psoas major to generate the contrast-to-noise ratio (CNR) curve. The kiloelectron-volt (keV) value corresponding to the highest point of the CNR curve was regarded as the optimal single energy of the measured ureter segment (*Figure 1*). Second, the CT images of the experimental group were processed to complete iodine-water material separation, and water-based images were taken as VNCT images.

All CT images were interpreted by two independent radiologists (both with 10 years of experience) blinded to the clinical information of both groups. Optimal Mono images of the nephrographic excretory phase from the experimental group and enhanced images of the excretory phase from the control group were selected for further measurement. The collecting system contralateral to the calculi was divided into seven segments: upper renal calyx (S1), lower renal calyx (S2), renal pelvis (S3), upper ureter (S4), middle ureter (S5), lower ureter (S6), and urinary bladder (S7). For each segment, radiologists placed three ROIs at proximal, middle, and distal parts of each segment of the urinary tract to obtain an average CT value ($CT_{urinary\ tract}$), which was a density value in Hounsfield units (HU). The CT value of the psoas major muscle and the standard deviation of the CT value of the abdominal subcutaneous fat at the umbilical level were measured in the same way, which represented the soft tissue CT value (CT_{soft}) and background noise (SD_{noise}), respectively. The CNR of each segment was calculated according to the following formula: $CNR = (CT_{urinary\ tract} - CT_{soft})/SD_{noise}$.

The volume-weighted CT dose index (CTDIvol),

Table 1 Patient demographics

Patient characteristics	Experimental group (n=24)	Control group (n=24)	P value
Male	20 (83%)	13 (54%)	0.029*
Age, yrs	45.25±14.30	45.38±11.55	0.369
Height, m	1.72±0.78	1.69±0.75	0.780
Weight, kg	70.58±14.05	72.79±12.91	0.569
BMI, kg/m^2	23.63±2.82	25.27±3.02	0.828

Values are presented as mean ± standard deviation or number (frequency). P values were calculated by the 2-sample *t*-test and the Pearson chi-squared test. BMI = weight (kg) / height * height (m^2). *, represents that the value was statistically significant. BMI, body mass index.

dose-length product (DLP), and the scanning range of the abdomen and pelvis (represented by L1 and L2, respectively; L1 and L2 were divided by the axial slice where the spina iliaca appeared) were recorded from the patient protocol of each CT scan. The effective dose (ED) was calculated in sections according to the following formula: ED = CTDIvol×(L1×0.015+L2×0.019). The values 0.015 and 0.019 were the effective dose weight factors of the abdomen and pelvis, respectively (7). The diameter of the calculi was measured from three orthogonal directions in the VNCT images of the experimental group and non-contrast images of the control group by two radiologists, and, finally, the maximum diameter of the calculi was recorded.

Statistical analysis

All data were analyzed using the software SPSS 23.0 (IBM Corp., Armonk, NY, USA). Categorical variables were presented as frequencies and percentages. Continuous variables in accordance with normal distribution were presented as means ± standard deviations. Other data were presented as the median (25th percentile; 75th percentile). An independent samples *t*-test was performed to compare demographic information and radiation dose between the two groups. The Mann–Whitney U test was used to compare the CT value, the CNR in each segment of the collecting system on the opposite side of the calculi, and the mean size of the calculi between the two groups. A P value <0.05 was considered indicative of a statistically significant difference.

Results

The demographic information of the experimental group (n=24) and the control group (n=24) is shown in *Table 1*. Three segments of the urinary tract in the experimental group (1.7%) and 4 segments in the control group (2.3%) were excluded due to insufficient filling. Finally, 165 segments from the experimental group and 164 segments from the control group were involved in further analysis.

Using GSI Viewer for postprocessing, CTU images of different single energy levels were observed, ranging from 40 to 140 keV. The CT value of the urinary tract gradually increased when single energy changed from high to low (*Figure 2*). The optimal single energy of the experimental group ranged from 48 to 58 keV, with an average of 52.1±2.21 keV.

The average CT values of each segment measured on the images of both groups are shown in *Table 2*. The CT values of each segment, except S7, in the experimental group were slightly lower than those in the control group, but the difference was not statistically significant (Z=–1.009 to –0.113; P>0.05).

The average CNRs calculated on optimal Mono images of the nephrographic excretory phase in the experimental group and images of the excretory phase in the control group are shown in *Table 3*. The CNR of the experimental group was lower than that of the control group, but the difference was not significant (Z=–0.999 to –0.309; P>0.05).

The radiation dose of CT scans of the two groups are shown in *Table 4*. The mean DLP of the experimental group was significantly lower than the total of the mean DLP in the three phases of the control group (784.61±62.27 *vs.* 1,266.71±613.03 mGy·cm; t=–3.833; P=0.001). Similarly, the experimental group had a lower mean ED than the control group (13.31±1.01 *vs.* 21.65±10.40 mSv; t=–3.909; P=0.001).

A total of 82 calculi were detected in the two groups.

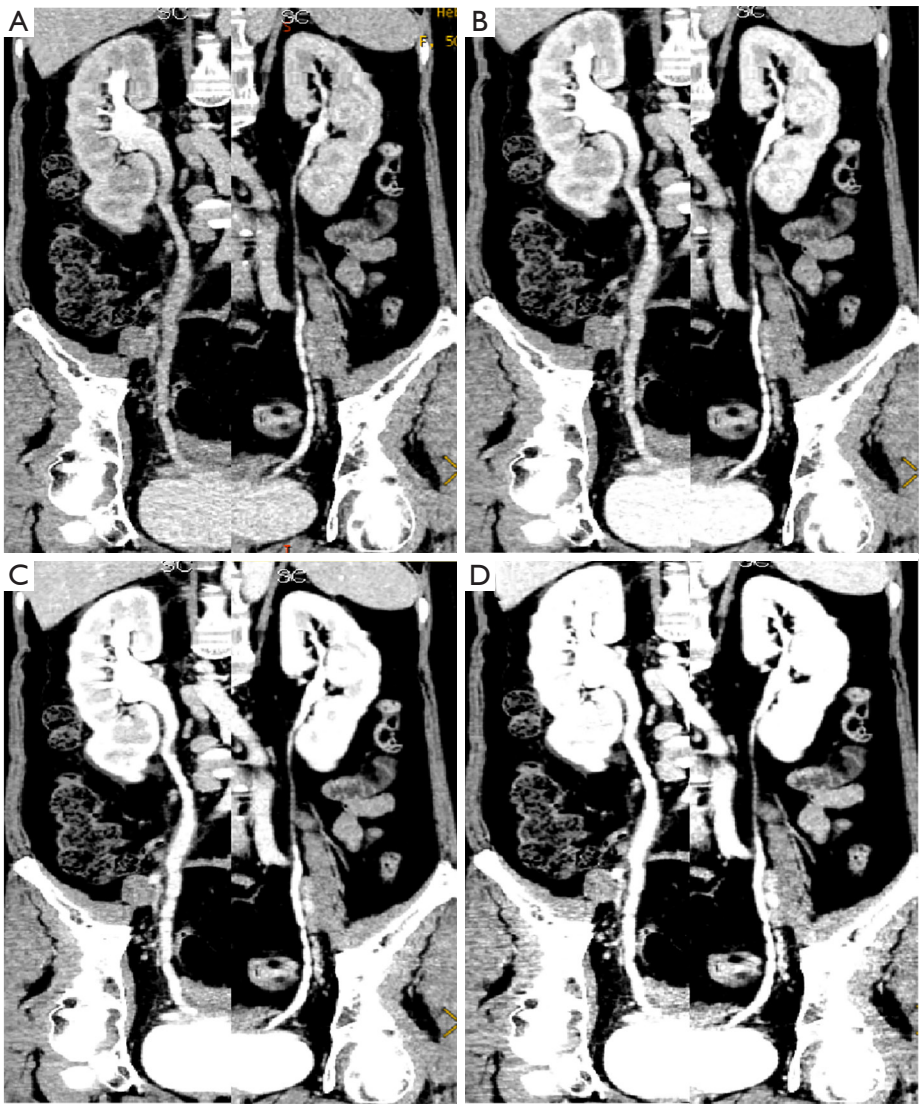

Figure 2 Monochromatic images. The coronal monochromatic images reconstructed at the single energy of 90 keV (A), 80 keV (B), 70 keV (C), and 60 keV (D), respectively, showing that the CT values of the urinary tract increased significantly with the decrease of the single energy. CT, computed tomography.

In the experimental group, 35 unilateral calculi covered by contrast medium were detected (*Figure 3*). The mean size of the calculi was 8.4 (6.0 to 11.0) mm. The locations of the calculi were the kidney (n=13), the ureter (n=17), the ureterovesical junction (n=3), and the prostatic urethra (n=2). In the control group, 47 unilateral calculi with an average size of 4.0 (1.0 to 2.0) mm were detected. The locations of the calculi were the kidney (n=30), the ureter (n=16), and the ureterovesical junction (n=1). Calculi detected in the control group had a smaller size than in the experimental group (Z=–3.282; P=0.001).

Discussion

One of the most common causes of hematuria in clinical practice is urolithiasis, which is always accompanied by acute renal colic as an emergency condition. The traditional urinary system modalities, including kidney-ureter-bladder radiography, and intravenous and ascending urography, have played an important role in urinary tract evaluation in the past century. In 1985, Zaontz's (8) research first applied CTU to the evaluation of the urinary system, making it possible to acquire a full anatomical presentation alongside

Table 2 The computed tomography values of each segment between the two groups

Segments	Experimental group	Control group	Z value	P value
S1	296.1±111.5	318.3±140.8	–0.113	0.910
S2	273.7±94.4	328.7±162.4	–0.825	0.409
S3	314.2±119.0	366.1±208.2	–0.598	0.550
S4	249.4±68.3	307.7±159.5	–0.639	0.523
S5	224.9±66.5	274.6±130.1	–1.002	0.307
S6	240.7±73.4	286.6±125.6	–1.009	0.313
S7	262.5±63.4	251.2±92.0	–0.680	0.496

Values are presented as mean ± standard deviation. S1, upper renal calyx; S2, lower renal calyx; S3, renal pelvis; S4, upper ureter; S5, middle ureter; S6, lower ureter; S7, urinary bladder.

Table 3 The CNR measurements for each segment between the two groups

Segments	Experimental group	Control group	Z value	P value
S1	12.1±6.2	12.8±6.5	–0.309	0.757
S2	10.8±5.2	13.5±8.4	–0.969	0.332
S3	13.1±6.6	15.9±13.4	–0.459	0.621
S4	9.6±4.3	12.6±9.7	–0.928	0.353
S5	8.3±3.9	11.2±8.6	–0.999	0.318
S6	9.2±4.5	11.7±8.4	–0.962	0.336
S7	10.1±4.0	9.3±4.0	–0.557	0.578

Values are presented as mean ± standard deviation. S1, upper renal calyx; S2, lower renal calyx; S3, renal pelvis; S4, upper ureter; S5, middle ureter; S6, lower ureter; S7, urinary bladder. CNR, contrast-to-noise ratio.

Table 4 Radiation dose of computed tomography scans

Radiation dose	Experimental group	Control group		
	Mixed nephrographic excretory phase DECT	Non-contrast CT	Nephrographic phase	Excretory phase
CTDIvol (mGy)	23.56	13.32±6.30	12.67±6.46	13.65±6.52
DLP (mGy·cm)	784.61±62.27	433.75±214.65	400.23±212.39	432.73±212.51
ED (mSv)	13.31±1.01	7.41±3.64	6.84±3.61	7.40±3.61

Values are presented as mean ± standard deviation. DECT, dual-energy computed tomography; CT, computed tomography; CTDIvol, volume weighted CT dose index; DLP, dose-length product; ED, effective dose.

convincing diagnostic information. Although a non-contrast CT scan is generally the first choice for diagnosing urinary calculi, it cannot provide information about renal function when a urinary obstruction is present. Urologists prefer to see the overall view of not only the location and size of the calculi but also the renal excretion function. CTU, consisting of a non-contrast, nephrographic, and excretory phase, is recommended as a one-stop tool for assessing the urinary tract anatomy prior to stone treatment (9).

Improvement of CTU for effective dose reduction

With increasing evidence that the increase of medical radiation dose correlates with the occurrence of malignant

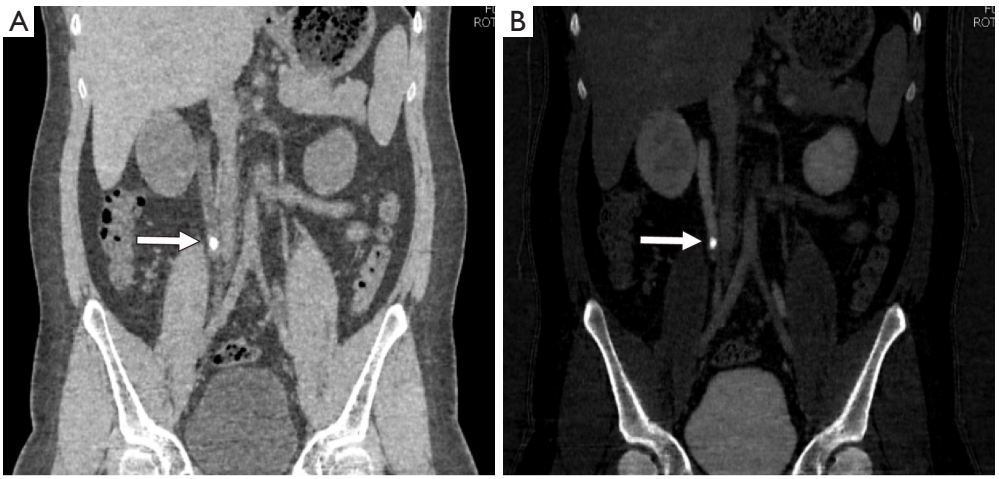

Figure 3 Material separation of DECT. The coronal images were water-based images (virtual non-contrast CT) (A) and iodine-based images (B). These images showed that calculi presented as high-density in the middle urinary tract (white arrows). DECT, dual-energy computed tomography.

tumors (10), there is increasing attention on CT radiation dose. CTU, which requires a non-contrast scan and multiple contrast scans according to the technical principle, is currently the abdominal examination technique with the most scanning phases and the highest radiation dose. Therefore, reducing the effective radiation dose of CTU examinations remains a major challenge for radiologists. Many studies, while attempting to decrease the radiation dose in different ways, have mainly focused on two aspects. First, the potential or current of the tube can be reduced if the multiple phases of CTU cannot be omitted. Zhang *et al.* (11) compared the ED of CTU after reducing the tube potential based on stratification of the patients' body mass index (BMI). They found that, for patients whose BMI was lower than 20, with the reduction of the tube potential from 100 to 80 kV, the ED decreased by about 31%. For patients whose BMI was between 20 and 30, the ED decreased by about 33% when the tube potential was reduced from 120 to 100 kV. The tube current was mostly reduced to 100–120 mAs in studies that focused on reducing the radiation dose. Further, Yang *et al.* (12) minimized the tube current to 80 mAs, which reduced the radiation dose by about 59% and had higher diagnostic efficiency for non-calculous urinary tract obstructive diseases. Second, the radiation dose can be reduced by reducing phase acquisitions (3,13). Using two-phase CTU with a split-bolus technique reduced two acquisitions of the whole urinary tract compared to traditional CTU. However, renal cortical phase images acquired at the angiographic phase that could evaluate the renal artery could not be obtained using the split-bolus technique. This could affect further characterization of renal space-occupying lesions, leading to the missed diagnosis of renal vascular lesions. Therefore, this method is only recommended if renal parenchymal space-occupying lesions or vascular lesions have been excluded.

In the control group of the present study, single-bolus three-phase CTU using a non-contrast scan during the nephrographic phase and the excretory phase reduced one phase acquisition and then reduced ED compared with a routine CTU of the urinary system. In the experimental group, a mixed nephrographic excretory phase CTU with a split-bolus technique reduced the number of acquisitions by three times compared with a routine CTU of the urinary system, which reduced ED by nearly 40% compared with the control group. Since all the patients in this study had urolithiasis, and patients with space-occupying lesions of the urinary tract were excluded, the design of the scan protocol was reasonable.

DECT and VNCT

The initial application of DECT to clinical practice occurred in the 1970s, but its clinical application was limited due to low spatial and density resolution, long scanning time, and poor output energy under low potential (14-16). In recent years, DECT has developed rapidly in many aspects, including the development of multi-slice spiral CT,

the improvement of spatial, density, and temporal resolution, and the improvement of post-progressing (17,18). At the same time, concerns about reducing radiation doses and how to maximize the value of DECT in reducing ED have gradually become the focus of medical professionals.

In this study, material separation of DECT was used to indirectly reduce ED. The DECT does not use a specific substance as a matrix for material separation, but rather chooses any two substances for separation. To ensure the accuracy and effectiveness of material separation, the main components of the tissue with large attenuation differences are generally paired, such as water and iodine, water and calcium, or calcium and iodine (19). In the present study, water-based images were obtained through material separation of iodine and water. The water-based images, which removed the iodine contrast medium in the urinary tract, could specifically show the components containing water. Similar to the non-contrast images, this technique is also called VNCT and can show calculi covered by a high-density contrast medium. Research shows that the VNCT of DECT has high sensitivity and specificity in detecting calculi. In an *in vitro* study by Stolzmann *et al.* (20), the specificity, sensitivity, negative predictive value, and positive predictive value of DECT in the detection of urate calculi *in vitro* were all 100%. In addition, Shuai *et al.* (21) found that the accuracy of detecting urinary calculi on virtual non-contrast images was 90%. The VNCT had the same capacity for detecting calculi larger than 4 mm as a conventional non-contrast scan. However, calculi smaller than 4 mm could not be displayed on VNCT images. In our study, although the positive rate of detecting calculi was not compared between VNCT images and other phase images in the experimental group, calculi were detected in all patients in the experimental group by VNCT. Further, calculi smaller than 4 mm were also detected, and the smallest diameter of calculi was 2.1 mm, which suggested that VNCT could be able to detect calculi smaller than 4 mm. Additionally, VNCT images of the experimental group showed all calculi detected by ultrasound and provided information of location and adjacent relations of high-density calculi, indicating that the VNCT scan could replace the conventional non-contrast scan in detecting urinary calculi.

Split-bolus single-phase CTU + VNCT = ED reduction

In this study, there was no significant difference between the CT values of the urinary tract contralateral to calculi in the experimental group and the control group. Moreover, the CT values of the experimental group were slightly lower than those of the control group except for the bladder, but there was no significant difference in CNR between the two groups, which suggested the effect of imaging of the collecting system in the two groups was consistent. The VNCT method could detect calculi by removing the cover of the contrast medium and obtaining the same contrast effect as the CTU of the control group. The ED of the experimental group was 40% lower than that of the control group due to being reduced to two acquisitions of the urinary tract. Therefore, patients with clinically confirmed or suspected urinary calculi are recommended to undergo split-bolus nephrographic excretory phase CTU in a DECT, in which the X-ray radiation dose is greatly reduced.

Limitations

Owing to the factors of radiation dose and the use of a contrast medium, it was difficult to achieve self-control in this study, so all cases became inter-group controls. Although our study used a completely randomized grouping design and the demographic information (e.g., age, height, weight, and BMI) of patients in the two groups were not significantly different except for gender, there were still several limitations in the present study. First, our study only evaluated the value of the clinical application of single-phase CTU with the split-bolus technique in patients with urinary calculi or suspected calculi, and whether this CTU protocol has wider application values in other diseases of the urinary system still needs further study. Second, due to the differences in cardiac function, renal function, or hemodynamics, the time in which the contrast medium was excreted to the urinary tract of each patient was not completely consistent. Therefore, the data measured within the same scanning time window in this study were limited. Future studies should design the time window individually according to the cardiac and renal function of different patients to obtain more accurate measurements than those achieved in our study. Last, the CT value of urinary and CNR were evaluated for the imaging effect of CTU in this study. In further similar studies, subjective evaluation should be performed to improve the evaluation of the CTU imaging effect.

Conclusions

DECT combined with split-bolus nephrographic excretory

phase CTU can display the urinary calculi covered by a contrast medium through virtual non-contrast images. It also plays an important role in reducing the ED exposure of patients by ensuring the same high-quality imaging of each segment in the collecting system. In doing so, this method represents a win-win situation.

Acknowledgments

Funding: None.

Footnote

Conflicts of Interest: All authors have completed the ICMJE uniform disclosure form (available at https://qims.amegroups.com/article/view/10.21037/qims-22-372/coif). The authors have no conflicts of interest to declare.

Ethical Statement: The authors are accountable for all aspects of the work in ensuring that questions related to the accuracy or integrity of any part of the work are appropriately investigated and resolved. The study was conducted in accordance with the Declaration of Helsinki (as revised in 2013). This study was approved by Hebei General Hospital Ethics Committee (No. 2022054). Informed consent was provided by all individual participants.

References

1. Zhu C, Wang DQ, Zi H, Huang Q, Gu JM, Li LY, Guo XP, Li F, Fang C, Li XD, Zeng XT. Epidemiological trends of urinary tract infections, urolithiasis and benign prostatic hyperplasia in 203 countries and territories from 1990 to 2019. Mil Med Res 2021;8:64.
2. Silverman SG, Leyendecker JR, Amis ES Jr. What is the current role of CT urography and MR urography in the evaluation of the urinary tract? Radiology 2009;250:309-23.
3. Dillman JR, Caoili EM, Cohan RH, Ellis JH, Francis IR, Nan B, Zhang Y. Comparison of urinary tract distension and opacification using single-bolus 3-Phase vs split-bolus 2-phase multidetector row CT urography. J Comput Assist Tomogr 2007;31:750-7.
4. Hack K, Pinto PA, Gollub MJ. Targeted delayed scanning at CT urography: a worthwhile use of radiation? Radiology 2012;265:143-50.
5. Dahlman P, van der Molen AJ, Magnusson M, Magnusson A. How much dose can be saved in three-phase CT urography? A combination of normal-dose corticomedullary phase with low-dose unenhanced and excretory phases. AJR Am J Roentgenol 2012;199:852-60.
6. Botsikas D, Hansen C, Stefanelli S, Becker CD, Montet X. Urinary stone detection and characterisation with dual-energy CT urography after furosemide intravenous injection: preliminary results. Eur Radiol 2014;24:709-14.
7. Menzel H, Schibilla H, Teunen D. Guidelines on radiation dose on the patient. European Guidelines on Quality Criteria for Computed Tomography 2006; Chapter 1, Appendix I: 32-33.
8. Zaontz MR, Pahira JJ, Wolfman M, Gargurevich AJ, Zeman RK. Acute focal bacterial nephritis: a systematic approach to diagnosis and treatment. J Urol 1985;133:752-7.
9. Türk C, Petřík A, Sarica K, Seitz C, Skolarikos A, Straub M, Knoll T. EAU Guidelines on Diagnosis and Conservative Management of Urolithiasis. Eur Urol 2016;69:468-74.
10. Yecies T, Bandari J, Fam M, Macleod L, Jacobs B, Davies B. Risk of Radiation from Computerized Tomography Urography in the Evaluation of Asymptomatic Microscopic Hematuria. J Urol 2018;200:967-72.
11. Zhang XQ, Wang N, Cui S. Feasibility study of reducing tube potential based on body mass index in the CTU examination. J Hebei Medical University 2017; 38:1089-1093.
12. Yang P, Yang WW. Application of low-dose CTU in non-calculous obstructive urinary tract diseases. J Clinical Medicine & Engineering 2017; 24:889-890.
13. Maheshwari E, O'Malley ME, Ghai S, Staunton M, Massey C. Split-bolus MDCT urography: Upper tract opacification and performance for upper tract tumors in patients with hematuria. AJR Am J Roentgenol 2010;194:453-8.
14. Genant HK, Boyd D. Quantitative bone mineral analysis using dual energy computed tomography. Invest Radiol 1977;12:545-51.
15. Goldberg HI, Cann CE, Moss AA, Ohto M, Brito A,

Federle M. Noninvasive quantitation of liver iron in dogs with hemochromatosis using dual-energy CT scanning. Invest Radiol 1982;17:375-80.
16. Chiro GD, Brooks RA, Kessler RM, Johnston GS, Jones AE, Herdt JR, Sheridan WT. Tissue signatures with dual-energy computed tomography. Radiology 1979;131:521-3.
17. Zeng Y, Geng D, Zhang J. Noise-optimized virtual monoenergetic imaging technology of the third-generation dual-source computed tomography and its clinical applications. Quant Imaging Med Surg 2021;11:4627-43.
18. Dubief B, Avril J, Pascart T, Schmitt M, Loffroy R, Maillefert JF, Ornetti P, Ramon A. Optimization of dual energy computed tomography post-processing to reduce lower limb artifacts in gout. Quant Imaging Med Surg 2022;12:539-49.
19. Michael GJ. Tissue analysis using dual energy CT. Australas Phys Eng Sci Med 1992;15:75-87.
20. Stolzmann P, Scheffel H, Rentsch K, Schertler T, Frauenfelder T, Leschka S, Sulser T, Marincek B, Alkadhi H. Dual-energy computed tomography for the differentiation of uric acid stones: ex vivo performance evaluation. Urol Res 2008;36:133-8.
21. Shuai T, Li ZL, Deng LP, Yuan Y, Pan XL, Cheng W, Li WJ. The value of split-bolus 2-phase with virtual non-enhanced scan in CT urography. Sichuan Da Xue Xue Bao Yi Xue Ban 2012;43:588-91, 596.

Cite this article as: Liang F, Zhou R, Wang G, Lan Y, Lei S, Zhang S. Dual-energy computed tomography in reducing the effective radiation dose of computed tomography urography in patients with urinary calculi. Quant Imaging Med Surg 2023;13(4):2208-2217. doi: 10.21037/qims-22-372

